Homogeneous Green's function retrieval on field data using the Marchenko method

Joeri Brackenhoff, Jan Thorbecke and Kees Wapenaar

Summary

Retrieval of the homogeneous Green's function is often done using a single-sided boundary, even though the theory states that an enclosing boundary is required. In recent years the theory has been modified to create a single-sided representation. This is done by using the Marchenko method, to redatum the wavefield from the boundary to a virtual receiver location inside the medium. The results on synthetic data have been encouraging, but on field data this method is largely unproven, due to the fact that the Marchenko method assumes that the medium is lossless, which in practice it is not. We have shown how to apply the classical representation and that it does not deliver the desired result on the field data. We have also demonstrated how to apply the new representation on the field data and that the result has improved over the classical representation. We visualize the result as snapshots over a region of interest to show the propagation of the wavefield through the medium.

Introduction

The Marchenko method has been developed in recent years to overcome the limitation of single-sided access to the subsurface of the Earth for retrieving the full wavefield in the subsurface (Broggini and Snieder, 2012; Wapenaar et al., 2014; Ravasi et al., 2016; Singh et al., 2016). It allows the retrieval of a Green's function in the subsurface through the use of a measured reflection response and an estimation of the first arrival at a point in the subsurface. By doing this the received wavefield at the surface can be redatumed into the medium. Further use of the Marchenko method allows us to not only redatum the receivers of the response, but also the sources, which means the entire wavefield can be redatumed into the subsurface. It has been shown that by using this method the homogeneous Green's function at depth can be retrieved (Wapenaar et al., 2017), a Green's function that has been superposed with its time-reversal. While the method has worked very well on synthetic data, it is still not widely applied to field data. This is because the method is very sensitive to irregularties in the acquisition setup and, more importantly, because the method assumes the medium where the reflection response is measured is lossless. We will show what the effects of the limitations of the field are and that, by applying corrections to the data, we can apply the Marchenko method to a field dataset and retrieve an accurate homogeneous Green's function.

Theory

The homogeneous Green's function is defined as the Green's function superposed by its time-reversal:

$$G_h(\mathbf{x}_R,\mathbf{x}_S,t) = G(\mathbf{x}_R,\mathbf{x}_S,t) + G(\mathbf{x}_R,\mathbf{x}_S,-t), \tag{1a}$$

$$G_h(\mathbf{x}_R,\mathbf{x}_S,\omega) = G(\mathbf{x}_R,\mathbf{x}_S,\omega) + G^*(\mathbf{x}_R,\mathbf{x}_S,\omega) = 2\Re G(\mathbf{x}_R,\mathbf{x}_S,\omega), \tag{1b}$$

where $G(\mathbf{x}_R,\mathbf{x}_S,t)$ denotes a Green's function recorded at receiver location $\mathbf{x}_R$ due to a source at $\mathbf{x}_S$ at time t. $G_h(\mathbf{x}_R,\mathbf{x}_S,t)$ is the homogeneous Green's function, $G(\mathbf{x}_R,\mathbf{x}_S,\omega)$ is the frequency transform at angular frequency ω and $\Re$ denotes the real part. The Green's function is defined as having a derivative of a delta function as a source, therefore the source singularity at $t=0$ vanishes when using the homogeneous Green's function:

$$\left(\rho(\mathbf{x})\nabla\cdot\left(\frac{1}{\rho(\mathbf{x})}\nabla\right) - \frac{1}{c^2(\mathbf{x})}\partial_t^2\right)G_h(\mathbf{x}_R,\mathbf{x}_S,t) = 0, \tag{2}$$

where c indicates the velocity, and ρ the density of the medium. The homogeneous Green's function can be used for applications such as holographic imaging and inverse scattering. The classical representation of the method states that the homogeneous Green's function can be retrieved between any two location in the subsurface as long as the medium is enclosed by a boundary (Porter, 1970; Oristaglio, 1989). This representation can be written as:

$$G_h(\mathbf{x}_R,\mathbf{x}_S,\omega) = \oint_{\partial\mathbb{D}} \frac{-1}{j\omega\rho(\mathbf{x})}\{\partial_i G(\mathbf{x}_R,\mathbf{x},\omega)G^*(\mathbf{x},\mathbf{x}_S,\omega) - G(\mathbf{x}_R,\mathbf{x},\omega)\partial_i G^*(\mathbf{x},\mathbf{x}_S,\omega)\}n_i \mathrm{d}^2\mathbf{x} \tag{3}$$

where j denotes the imaginary unit and $\rho(\mathbf{x})$ denotes the density of the medium at location $\mathbf{x}$ and n_i is the normal vector. $\partial\mathbb{D}$ is a closed boundary around medium $\mathbb{D}$. In this equation $G^*(\mathbf{x},\mathbf{x}_S,\omega)$ can be seen as being a source distribution that works on the boundary $\partial\mathbb{D}$ at all $\mathbf{x}$. $G(\mathbf{x}_R,\mathbf{x},\omega)$ is a propagator that propagates the response from the boundary at $\mathbf{x}$ to $\mathbf{x}_R$. If the condition of having a closed boundary is not fulfilled, the result will contain artifacts and the retrieved homogeneous Green's function will be incorrect. In spite of this, the classical representation is still widely used, also for situations where there is no closed boundary, as there are few alternatives. In recent years, however, a promising new method has been developed, namely the Marchenko method. Unlike the classical representation it does not require a closed boundary (Wapenaar et al., 2014) and can retrieve the Green's function at any virtual receiver location in the subsurface without resolving the overburden (Broggini et al., 2012). The reason for this is because the method can handle internal multiples correctly, while primaries are handled in the same way as more conventional methods. The method requires an accurate reflection response measured at a single-sided surface of the medium and an estimation of the first arrival, which can be modeled in a smooth velocity model. In order to obtain the Green's function, the Marchenko method retrieves a focusing function $f_2(\mathbf{x}_R, \mathbf{x}, \omega)$, which operates in a medium that is truncated at $\mathbf{x}_R$ and focuses to that location. Wapenaar et al. (2017) showed that using the results of the Marchenko method, the homogeneous Green's function can be retrieved at any location in the medium using a single-sided boundary. This representation can be written as:

$$G_h(\mathbf{x}_R, \mathbf{x}_S, \omega) = -\Im \int_{\partial\mathbb{D}_0} \frac{4}{\omega\rho(\mathbf{x})} \{\partial_3 f_2(\mathbf{x}_R, \mathbf{x}, \omega) G(\mathbf{x}, \mathbf{x}_S, \omega)\} \mathrm{d}^2\mathbf{x}, \quad (4)$$

Similar to Eq.3, in this equation, one can see one function as the propagator and the other as a source. The focusing function $f_2(\mathbf{x}_R, \mathbf{x}, \omega)$ can be seen as the source, that works on the single-sided boundary and the Green's function $G(\mathbf{x}, \mathbf{x}_S, \omega)$ operates as the propagator, similarly to $G(\mathbf{x}_R, \mathbf{x}, \omega)$ in Eq.3. It propagates the response from the boundary at $\mathbf{x}$ to $\mathbf{x}_S$. By evaluating Eq.4 the response between the two locations is retrieved. This representation will not contain artifacts like the ones found when using the classical representation and will retrieve the accurate homogeneous Green's function.

Application on field data

In order to apply the method to field data, we need to go to several steps. First of all we require the input data for the Marchenko method. For this we use a field dataset in the Vøring basin, which was acquired in 1994 by SAGA Petroleum A.S., which at the time of writing is part of Statoil ASA. The data was preprocessed by Eric Verschuur, who removed the free-surface multiples and retrieved the near offsets using the EPSI method (Van Groenestijn and Verschuur, 2009). The reason that the free-surface multiples needed to be removed is because the Marchenko method that was applied cannot handle these multiples. There are schemes that are capable of doing this, for example the one found in Singh et al. (2016). The data was attenuated and had incorrect source strength, which we applied corrections for. In case these corrections are not done, they can lead to additional artifacts. There are ways to correct for attenuation (Alkhimenkov, 2017) and for incorrect source strength (Brackenhoff, 2016), but further research is required. In this case, the corrections were retrieved adaptively. The estimated smooth velocity model for the field data is shown in Fig.1-a, and an example of a shot after processing in Fig.1-b. Using the data in Fig.1, we retrieve Green's functions and focusing functions in the medium at two

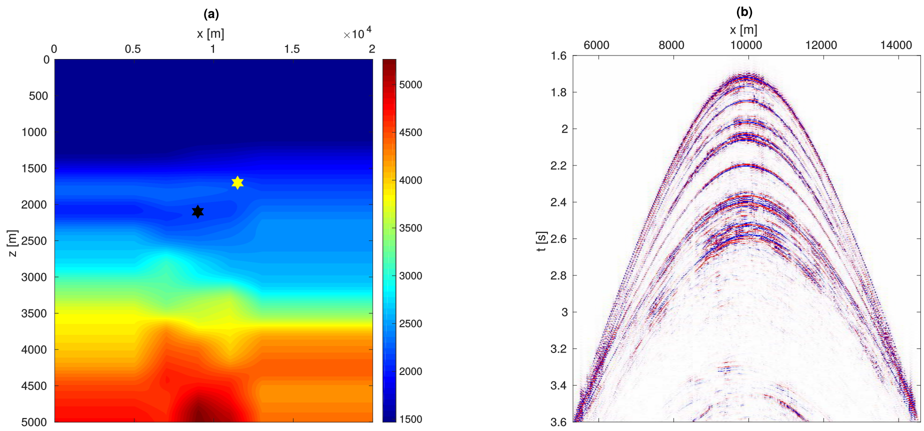

Figure 1 *(a) Estimated smooth velocity model of the subsurface used for estimating the first arrivals needed for the Marchenko scheme. The two stars indicate two different locations where the virtual receivers are retrieved. The yellow star is the virtual receiver location of the wavefield in Fig.2-a and the black star is the virtual receiver location of the wavefields in Fig.2-b and Fig.2-c. (b) Example of a single shot of the reflection response after corrections have been applied. The source wavelet and free-surface multiples have been removed using the EPSI method, which also estimated the near-offsets.*

separate locations using the Marchenko method, indicated by the stars in Fig.1-a. The Green's function that was retrieved at the location of the yellow star is shown in Fig.2-a and is used as $G(\mathbf{x}, \mathbf{x}_S, \omega)$ in Eq.3. The Green's function that was retrieved at the location of the black star is shown in Fig.2-b and is used as $G(\mathbf{x}_R, \mathbf{x}, \omega)$ in Eq.3. The resulting homogeneous Green's function is shown in Fig.2-d. An important property of the homogeneous Green's function has not been fulfilled with this result. The result is not symmetric in time, thereby violating the definition given in Eq.1a. Also note that, in this example, both

Green's function have been fully retrieved and therefore, the best possible result is achieved. If one of the Green's functions is less accurate, the homogeneous Green's function will be less accurate as well. We will use the focusing function next. Instead of the Green's function in Fig.2-b, we use the focusing function retrieved at the virtual receiver location, which is shown in Fig.2-c. We use this focusing function as $f_2(\mathbf{x}_R, \mathbf{x}, \omega)$ in Eq.4, while still using the Green's function from Fig.2-a as $G(\mathbf{x}, \mathbf{x}_S, \omega)$. The homogeneous Green's function that is retrieved is shown in Fig.2-e. This result is symmetric in time and contains several events that are similar to the ones found in Fig.2-d. The reason that the two results are similar is that the primaries are handled the same for both representations. Only the multiples are handled differently and therefore the result improves. This can be seen in the differences between the two homogeneous Green's functions. The result in Fig.2-e is only a single trace as it describes the response

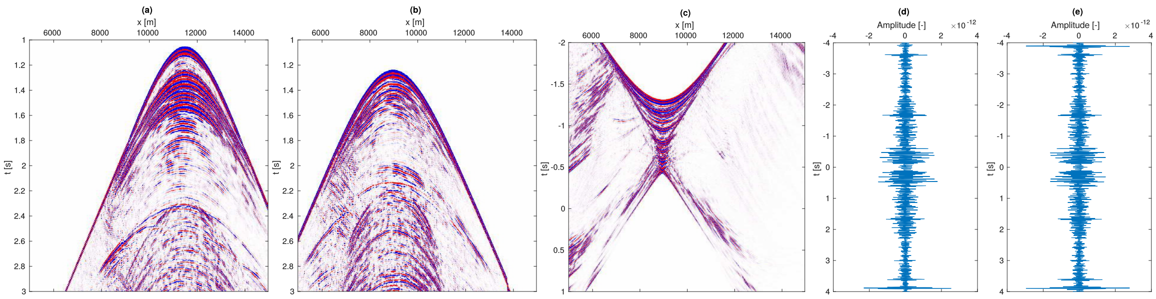

Figure 2 *(a) Green's function retrieved at the location of the yellow star in Fig.1-a and is used as $G(\mathbf{x}, \mathbf{x}_S, \omega)$ in Eq.3 and Eq.4. (b) Green's function retrieved at the location of the black star in Fig.1-a and is used as $G(\mathbf{x}_R, \mathbf{x}, \omega)$ in Eq.3. (c) focusing function retrieved at the location of the black star in Fig.1-a and is used as $f_2(\mathbf{x}_R, \mathbf{x}, \omega)$ in Eq.3 and Eq.4. (d) Homogeneous Green's function as a result of Eq.3 when using the wavefields in Fig.2-a and Fig.2-b as input. (e) Homogeneous Green's function as a result of Eq.4 when using the wavefields in Fig.2-a and Fig.2-c as input. All events were convolved with a 30 Hz Ricker wavelet.*

between two single locations. We have applied the result to many different locations all throughout the medium and retrieved the homogeneous Green's function at all of these locations. The location of the virtual receiver was varied, while the source was kept the same. The results are shown in Fig.3, where they are visualized as snapshots of the homogeneous Green's function. Due to the large amount of disk space required for storage, only the region of interest of the medium is shown. The first 1200 m mainly consists of seawater, therefore it is not shown. The background of the figure is an image of the subsurface retrieved using the Marchenko method. Starting at the source, the primary wavefield propagates through the medium and has a greater velocity at deeper depths, which corresponds with the velocity model. When the wavefield hits a boundary, a reflection is caused, which in turn causes additional reflections. There is noise present in the result, but the desired wavefield at depth has been captured.

Conclusions

We have shown that, using the Marchenko method instead of the classical representation, the homogeneous Green's function can be accurately retrieved. While this was done on synthetic data, we have shown that this is also possible on field data and that the new representation is indeed an improvement over the classical one. Due to the nature of the Marchenko scheme, there should be corrections applied to the reflection response before the Green's function and focusing function are retrieved. If this is done, the results on field data show the primary wavefield, as well as the coda. These results should be explored further and on more complex datasets. The results in 2D are encouraging enough that 3D data is a viable next step.

Acknowledgements

We thank Statoil ASA for the use of their data, Eric Verschuur for the pre-processing of the data and Joost van der Neut, Evert Slob, Myrna Staring, Christian Reinicke Urruticoechea, Lele Zhang and Ivan Vasconcelos for their insightful commentary on the work

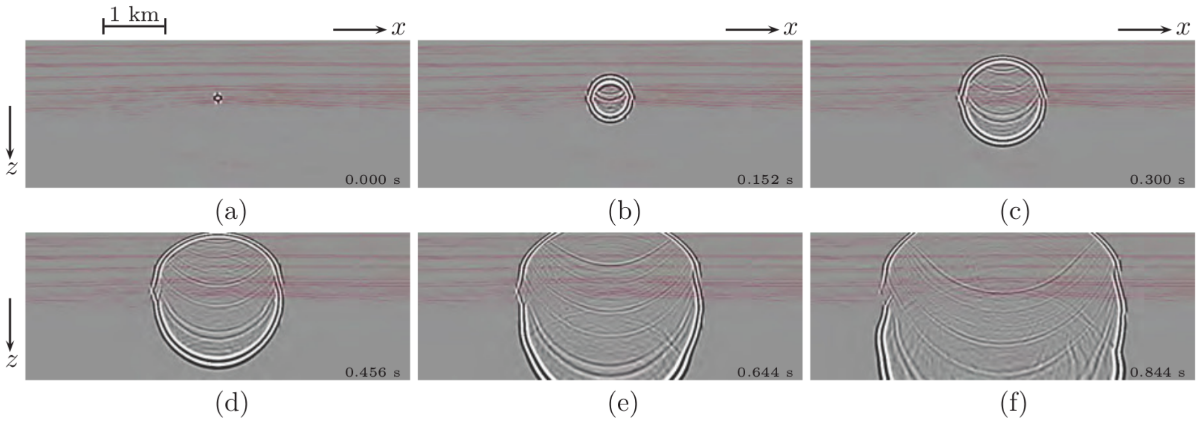

Figure 3 *Snapshots of the homogeneous Green's function on a field dataset in the Vøring basin at different times. The depth varies from 1200 to 3500 m and the offset varies from -3000 to 3000 m from the center. The wavefield has been convolved with a 30 Hz Ricker wavelet and the background is an image retrieved using the Marchenko method. Note, however, that for obtaining the snapshots we used the smooth background model of Fig.1-a*

References

Alkhimenkov, Y. [2017] Redatuming and Quantifying Attenuation from Reflection Data Using the Marchenko Equation: A Novel Approach to Quantify Q-factor and Seismic Upscaling. *TU Delft online repository*.

Brackenhoff, J. [2016] Rescaling of incorrect source strength using Marchenko redatuming. *TU Delft online repository*.

Broggini, F. and Snieder, R. [2012] Connection of scattering principles: A visual and mathematical tour. *European Journal of Physics*, **33**(3), 593.

Broggini, F., Snieder, R. and Wapenaar, K. [2012] Focusing the wavefield inside an unknown 1D medium: Beyond seismic interferometry. *Geophysics*, **77**(5), A25–A28.

Oristaglio, M.L. [1989] An inverse scattering formula that uses all the data. *Inverse Problems*, **5**(6), 1097.

Porter, R.P. [1970] Diffraction-limited, scalar image formation with holograms of arbitrary shape. *JOSA*, **60**(8), 1051–1059.

Ravasi, M., Vasconcelos, I., Kritski, A., Curtis, A., Filho, C.A.d.C. and Meles, G.A. [2016] Target-oriented Marchenko imaging of a North Sea field. *Geophysical Supplements to the Monthly Notices of the Royal Astronomical Society*, **205**(1), 99–104.

Singh, S., Snieder, R., van der Neut, J., Thorbecke, J., Slob, E. and Wapenaar, K. [2016] Accounting for free-surface multiples in Marchenko imaging. *Geophysics*.

Van Groenestijn, G. and Verschuur, D. [2009] Estimation of primaries and near-offset reconstruction by sparse inversion: Marine data applications. *Geophysics*, **74**(6), R119–R128.

Wapenaar, K., Thorbecke, J., Neut, J., Slob, E. and Snieder, R. [2017] Virtual sources and their responses, Part II: data-driven single-sided focusing. *Geophysical Prospecting*.

Wapenaar, K., Thorbecke, J., Van Der Neut, J., Broggini, F., Slob, E. and Snieder, R. [2014] Marchenko imaging. *Geophysics*, **79**(3), WA39–WA57.